DISCRETE AND CONTINUOUS
DYNAMICAL SYSTEMS SERIES B
Volume **16**, Number **4**, November **2011**

doi:10.3934/dcdsb.2011.16.xx

pp. **X–XX**

NUMERICAL SIMULATION OF TWO-FLUID FLOW AND MENISCUS INTERFACE MOVEMENT IN THE ELECTROMAGNETIC CONTINUOUS STEEL CASTING PROCESS

B. Wiwatanapataphee and T. Mookum

Department of Mathematics, Faculty of Science
Mahidol University
Bangkok, 10400, THAILAND

Y. H. Wu

Department of Mathematics and Statistics
Curtin University of Technology
Perth, WA, 6845, AUSTRALIA

(Communicated by the associate editor name)

Abstract. This paper presents a mathematical model and numerical technique for simulating the two-fluid flow and the meniscus interface movement in the electromagnetic continuous steel casting process. The governing equations include the continuity equation, the momentum equations, the energy equation, the level set equation and two transport equations for the electromagnetic field derived from the Maxwell's equations. The level set finite element method is applied to trace the movement of the interface between different fluids. In an attempt to optimize the casting process, the technique is then applied to study the influences of the imposed electromagnetic field and the mould oscillation pattern on the fluid flow, the meniscus shape and temperature distribution.

1. **Introduction.** Electromagnetic (EM) continuous casting is an industrial heat extraction process for converting molten steel to steel products. In the EM casting process, molten steel is continuously poured into a water-cooled mould where intensive cooling causes a thin solidified steel shell to form around the edge of the steel, and the solidified steel is continuously withdrawn from the bottom of the mould. To prevent the molten steel from oxidation and sticking to the mould wall, mould powder or lubricant fluid is added on the top of the mould and the mould oscillates vertically for the lubricant fluid to form a layer on the top of the molten steel and between the mould wall and the steel. Electromagnetic field is also imposed on the system to control the flow pattern of fluids in the mould and the solidification process particularly in the meniscus region, as it has been recognized that the surface quality of the casting products is mainly associated with the phenomena in the meniscus region.

2000 *Mathematics Subject Classification.* Primary: 74A50; Secondary: 74S05.

Key words and phrases. Electromagnetic caster, continuous steel casting process, meniscus shape, two-fluid flow, level set method, finite element method.

The authors is supported by the OHEC and the TRF through the RGJ Ph.D. Program grant PHD/0212/2549.

To achieve high production rate and ensure high quality of the casting products, intensive studies have been carried out worldwide over the last few decades to model various aspects of the continuous casting process, in particular the heat transfer - solidification process [10, 27], the flow phenomena [22, 25], the electromagnetic stirring [12, 14, 15, 21] and formation of oscillation marks [11]. However, as analyzed by Thomas [23], the continuous casting process involves a staggering complexity of at least 18 interacting phenomena at the mechanic level, and due to the complexity, previous work mainly focus on each individual phenomena or interaction of two or three phenomena only. On the other hand, to have optimal control of the casting process, it is essential to fully understand the interaction of the main physical phenomena occurring in the casting process. Hence, development of sophisticated models capable of simulating the staggering complexity of the major interacting phenomena including the heat transfer, phase change, electromagnetic stirring, fluid flow and evolution of the interface between different fluids is still a challenge.

In this work, we further develop our previous works [25, 29] in various aspects. In [25], an enthalpy finite element method was developed to model the interacting phenomena of heat transfer, solidification and turbulence in the casting process. The work of [29] extend the model of [25] by incorporating the effect of the electromagnetic field in the coupled heat transfer - turbulence flow model. In this paper, we generalize the previous models to include the mould oscillation effect and the interaction between the lubricant fluid and the molten steel. With this generalization, it becomes possible to simulate and quantitatively analyze the complex interacting phenomena occurring in the meniscus region of the casting mould, particularly the meniscus interface movement and the influence of the mould oscillation pattern. The rest of the paper is organized as follows. In section two, the complete set of equations for the model is established. In section three, the method of solution is described briefly. In section four, a numerical study is presented.

2. **Mathematical Model.**

The EM casting process involves various complex physical phenomena including heat transfer with phase change, electromagnetic stirring, fluid flow and evolution of the interface between the lubricant fluid and the molten steel. These phenomena interact each other. For the lubricant fluid - molten steel flow problem, the key modeling element is the tracking of the evolution of the interface between the two fluids in the dynamic casting process. Many techniques may be used for solving this kind of problems such as the Arbitrary Lagrangian-Eulerian method [5, 7, 17] and the level set method [16]. In this work, we develop an algorithm based on the conservative level set method in which the interface is defined as a ϕ_0 level of a level set function, namely

$$\tau_{int} \;=\; \{(x, y, z) \in R^3 : \phi(x, y, x, t) = \phi_0\}$$

The level set function is set to zero in the molten steel, $\phi_0 = 0.5$ on the interface and one in the lubricant fluids. When the fluids flow with velocity $\mathbf{v}$, the level set function evolves with time according to the following convection-diffusion equation

$$\frac{\partial \phi}{\partial t} + \mathbf{v} \cdot \nabla \phi = \gamma \nabla \cdot [\varepsilon \nabla \phi - \phi(1 - \phi)\mathbf{n}] \tag{1}$$

where γ is a reinitialization parameter and ε is the thickness of the interface, and $\mathbf{n} = \frac{\nabla \phi}{|\nabla \phi|}$ is the unit normal vector on the interface [18].

To construct the governing equations for the flow of both fluids in a unified form, let

$$\rho = \rho_s + (\rho_o - \rho_s)\phi, \tag{2}$$
$$\mu = \mu_s + (\mu_o - \mu_s)\phi, \tag{3}$$
$$c = c_s + (c_o - c_s)\phi, \tag{4}$$
$$k = k_s + (k_o - k_s)\phi, \tag{5}$$

where the subscripts s and o denote respectively molten steel and lubricant fluid. Thus, in terms of the ρ, μ, c and k defined above, the flow of both the lubricant fluid and the molten steel can be expressed in vector form as follows.

$$\nabla \cdot \mathbf{v} = 0 \tag{6}$$

$$\frac{\partial \mathbf{v}}{\partial t} - \nabla \cdot \left(\frac{1}{R_e} \nabla \mathbf{v} - \mathbf{v}\mathbf{v} - \frac{1}{\rho} p \mathbf{I} \right) = \mathbf{g} + \frac{1}{\rho} \mathbf{F}_{em} + \frac{1}{\rho} \mathbf{F}_{st}, \tag{7}$$

where p is pressure, $\mathbf{g}$ is the gravitational acceleration, $\mathbf{v}$ denotes the fluid velocity, $R_e > 0$ denotes the Reynolds number. The forcing function $\mathbf{F}_{em}$ is the EM force which, from our previous work in [1], can be calculated by

$$\mathbf{F}_{em} = \mathbf{J} \times (\nabla \times \mathbf{A}), \tag{8}$$

where $\mathbf{A}$ and $\mathbf{J}$ denote respectively the magnetic vector potential and current density. In [1], it has been demonstrated that from the Maxwell's equations, by neglecting the influence of the displacement current and the flow induced current on the magnetic field, $\mathbf{A}$ and $\mathbf{J}$ are governed by the following trnasport equations

$$\nabla \times (\frac{1}{\nu} \nabla \times \mathbf{A}) = \mathbf{J}, \tag{9}$$
$$\nabla \cdot \mathbf{J} = 0, \tag{10}$$

where $\mathbf{J} = \mathbf{J}_s - \eta \nabla \varphi$, ν and η denote respectively the magnetic permeability and electroconductivity, $\mathbf{J}_s$ is the source current density, and φ is a scalar potential function.

The forcing function $\mathbf{F}_{st}$ is the surface tension force acting only on the interface and is given by Brackbill et al. [3] and Chang et al. [4] by

$$\mathbf{F}_{st} = \sigma \delta(\phi) \kappa(\phi) \mathbf{n}, \tag{11}$$

where σ and $\delta(\phi)$ denote respectively the surface tension coefficient and the delta function, $\kappa(\phi) = -\nabla \cdot \mathbf{n}$ is the interfacial curvature. The smooth delta function for the simulation here is chosen to be

$$\delta(\phi) = 6|\nabla \phi||\phi(1-\phi)|. \tag{12}$$

For the problem of heat transfer with phase change occurring in the casting process, we utilize the single domain enthalpy method developed in our previous work [28] as one of the elements toward tacking of the coupled problems in question. In this method, the temperature field is governed by the following energy equation

$$\frac{\partial T}{\partial t} + \nabla \cdot (\mathbf{v}T - \alpha \nabla T) = S_T, \tag{13}$$

where T is temperature, $\alpha = k/\rho$ is the thermal diffusivity, and S_T is the heat source due to phase change and is zero everywhere except in the mushy region of

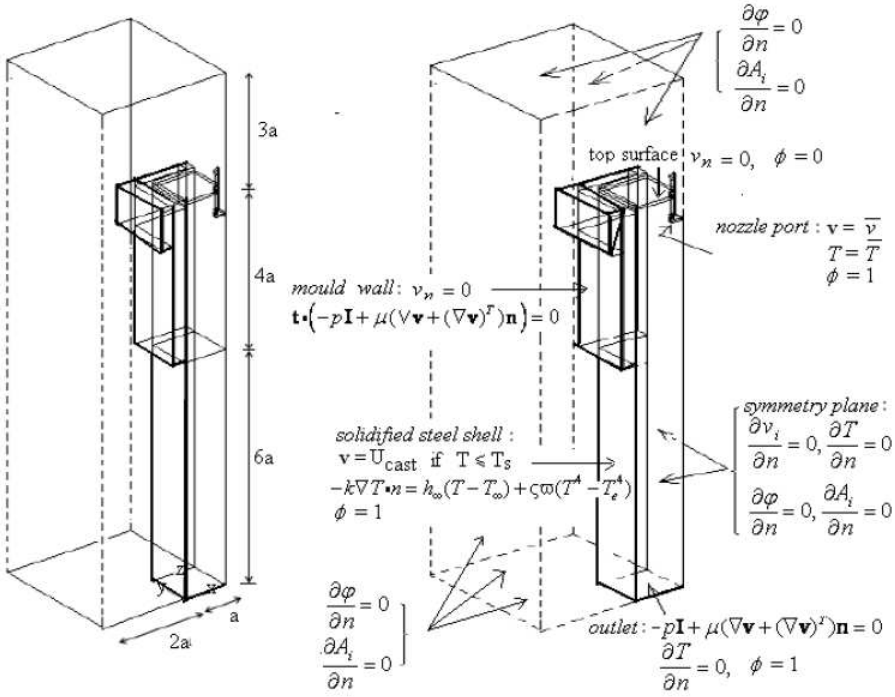

FIGURE 1. Computation domain (a=0.1 m.) and boundary conditions.

steel where

$$S_T = -\frac{1}{c}\left(\frac{\partial H_L}{\partial t} + \mathbf{v}\cdot\nabla H_L\right)(1-\phi). \tag{14}$$

Here H_L denotes the enthalpy function which can be approximated by the linearly distributed function of temperature namely $H_L = Lf(T)$ in which L is the latent heat of liquid steel and $f(T)$ is liquid fraction. The liquid fraction is zero in the solidified region, one in the liquid region and can be approximated as a linear function of temperature in the mushy region namely

$$f(T) = \begin{cases} 0 & \text{if } T \leq T_S, \\ \dfrac{T - T_S}{T_L - T_S} & \text{if } T_S < T < T_L, \\ 1 & \text{if } T \geq T_L, \end{cases} \tag{15}$$

where T_S and T_L are respectively the solidification temperature and melting temperature of the steel.

Equations (1) - (16) constitute a system of ten partial differential equations in terms of six coordinates and time-dependent unknown functions v_x, v_y, v_z, p, T and ϕ and four time-independent unknown functions $\mathbf{A} = (A_x, A_y, A_z)$ and φ. To completely define the problem, we specify the boundary conditions for the velocity field, temperature field, level set function and EM field as shown in Figure 1.

3. **Method of Solution.** The electromagnetic field problem as shown in section two can be uncoupled from the two-fluid flow and heat transfer problem. Thus, the electromagnetic field problem governed by (9) and (10) is solved first for $\mathbf{A}$ and φ

by using the standard Galerkin finite element method to yield the electromagnetic force for the subsequent two-fluid flow and heat transfer analysis.

We thus have the closed system of six partial differential equations in terms of six coordinates and time dependent unknown functions (v_x, v_y, v_z, p, T, and ϕ). A numerical algorithm based on the finite element method is then developed to solve the coupled problem. The fractures of the algorithm include: using the penalty function method to weaken the continuity requirement for the fluid flow problem; using a single domain enthalpy method to track the interface between the lubricant fluid and the molten steel; using the Galerkin finite element method for discretization in space. To keep detail of the paper to a minimum, the lengthy formulation is omitted here. The resultant equations after discretization in space can be expressed by

$$M\dot{\mathbf{q}} + K\mathbf{q} = \mathbf{f}, \tag{16}$$

where $\mathbf{q} = (\mathbf{U}, \mathbf{P}, \mathbf{T}, \Phi)$ represents the values of the corresponding unknown at the nodes of the finite element mesh. The matrix M corresponds to the transient terms in the governing partial differential equations. The matrix K corresponds to the advection and diffusion terms, and the vector $\mathbf{f}$ depends nonlinearly on $\mathbf{U}$ and Φ.

The numerical solutions to the nonlinear discretization system are then obtained by using an iterative scheme developed based on Euler's backward scheme. The following convergent condition was used in the simulation

$$\|R_i^{m+1} - R_i^m\| \leq Tol, \tag{17}$$

where the subscript $m+1$ and m denote iterative computation steps, R_i denotes the solution vector of the ith variable on the finite element nodes, $\|\cdot\|$ is the Euclidean norm and Tol is a small positive constant.

4. **Numerical Investigation and Discussion.** We study here the three-dimensional two-fluid flow and heat transfer process in the continuous steel casting. The example under investigation is a square caster with size $0.2 \times 0.2 \times 0.4\ m^3$, and a submerged entry nozzle with port outlet angle of 15^o downward. The computation region, as shown in Figure 1, represents just one quadrant of the casting steel system consisting of the strand region occupied by the steel and lubricant oil on the top, the mould region surrounding by mounted coil and the environment region. The finite element mesh with finer grid around the meniscus region, used in this study, consists of 16,478 tetrahedral elements with a total of 133,437 degrees of freedom. The values of model parameters used in this simulation are listed in Table 1.

With the EM field, $\mathbf{A}$ and φ, determined, we can determine the current density vector $\mathbf{J}$, the magnetic flux density vector $\mathbf{B}$ and the EM force $\mathbf{F}_{em}$. Figure 2 shows the $\mathbf{J}$, $\mathbf{B}$ and $\mathbf{F}_{em}$ fields. The results show that the current density circulates in a clockwise direction parallel to the horizontal plane and the magnetic flux density flows downward and parallel to the vertical plane, while the EM forces act on the molten steel basically in the horizontal direction toward the central line.

Figure 3 shows the pattern of molten steel flow on a symmetry plane. It is noted that molten steel leaving the nozzle as a strong hot jet hits the top part of the mould wall and then splits into two parts respectively in upward and downward directions. This leads to two recirculation zones including an upper small recirculation zone below the meniscus and a lower big recirculation zone below the nozzle port. The comparison indicates that the EM force is an important factor dominating the velocity field and the meniscus shape on the top region of the mould wall. The

TABLE 1. Parameters used in numerical simulation

Parameters	Value	Unit
Delivery velocity of molten steel u_{in}	0.12	m/s
Density of molten steel ρ_s	7800	kg/m^3
Density of lubricant oil ρ_o	2680	kg/m^3
Effective viscosity of molten steel μ_s	0.001	$Pa \cdot s$
Effective viscosity of lubricant oil μ_o	0.321	$Pa \cdot s$
Surface tension coefficient σ	1.6	m/s^2
Thickness of the interface ε	0.001	m
Gravitational acceleration g	-9.8	m/s^2
Pouring temperature T_{in}	1535	^oC
Molten steel temperature T_L	1525	^oC
Solidified steel temperature T_S	1465	^oC
Shell surface temperature T_∞	150	^oC
Environment temperature T_e	100	^oC
Mould wall temperature T_m	1400	^oC
Heat capacity of molten steel c_s	465	J/kg^oC
Heat capacity of lubricant oil c_o	1000	J/kg^oC
Thermal conductivity of molten steel k_s	35	W/m^oC
Thermal conductivity of lubricant oil k_o	1	W/m^oC
Latent heat of liquid steel L	2.72×10^5	J/kg
Heat transfer coefficient of molten steel h_∞	1079	$W/m^{2o}C$
Amplitude of mould oscillation A	0.02	m
Angular frequency of mould oscillation ω	$150(2\pi/60)$	rad/s
Emissivity of solid steel ϖ	0.4	
Stefan-Boltzmann constant ς	5.66×10^{-8}	W/m^2K^4
Magnetic permeability of vacuum ν	$4\pi \times 10^{-7}$	Henry/m
Electric conductivity of steel η_s	4.032×10^6	
Electric conductivity of coil η_c	1.163×10^7	
Electric conductivity of air η_a	10^{-39}	
Source current density $\lvert\mathbf{J}_s\rvert$	2×10^5	A/m^2

velocity field around the meniscus region as shown in Figure 4 indicates that the EM force leads to the reduction of flow speed especially in the top region near the mould wall. The EM force thus contributes to preventing molten steel from sticking to the mould wall and smoothing the steel casting surface.

Figures 5 and 6 compare the interfaces ($\phi = 0.5$) obtained from the model with EM force and with no EM force. The results show that the EM force gives an expanded and weakened upper recirculation zone near the mould wall, and deeper interface around the billet corner.

Figures 7-9 show temperature distributions in the continuous steel casting. The results indicate that the temperature field is more uniform with the EM forces and that the electromagenetic field can be used to control the solidification process.

To investigate the effect of the mould oscillation, we study the dynamic phenomena occurring in a complete mould oscillation cycle. Figure 10 gives the pattern of the mould oscillation and various instants of time for which the dynamic phenomena is to be presented. Figure 11 plots the velocity field on the symmetry plane at various instants of time during an oscillation cycle of the mould. It is indicated that

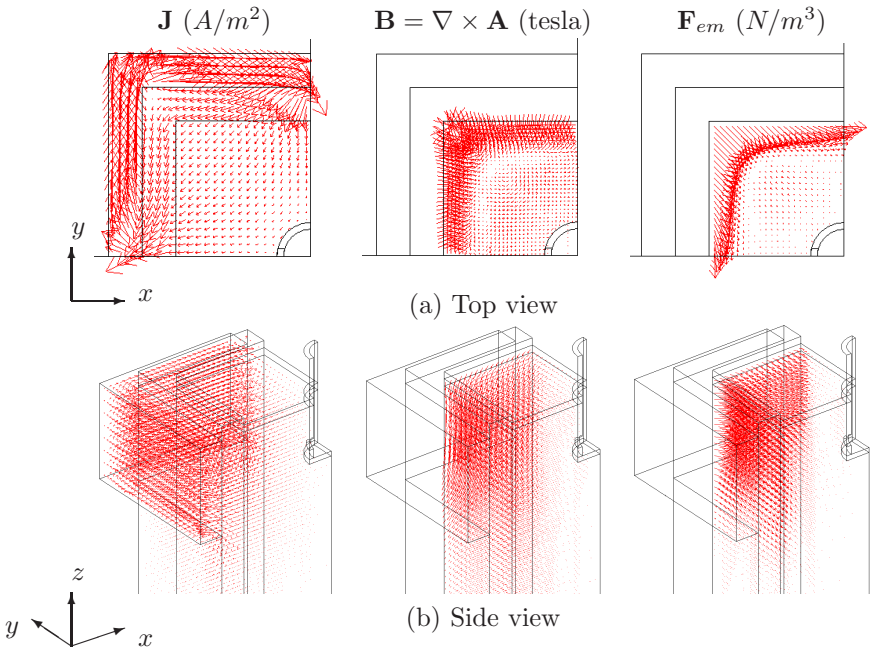

FIGURE 2. Simulated solutions of: the current density $\mathbf{J}$ (A/m^2) in the coil, mould and molten steel pool (first column); the magnetic flux density $\mathbf{B}$ (tesla) in the molten steel pool (second column); and the EM force $\mathbf{F}_{em}$ (N/m^3) in the molten steel pool (third column).

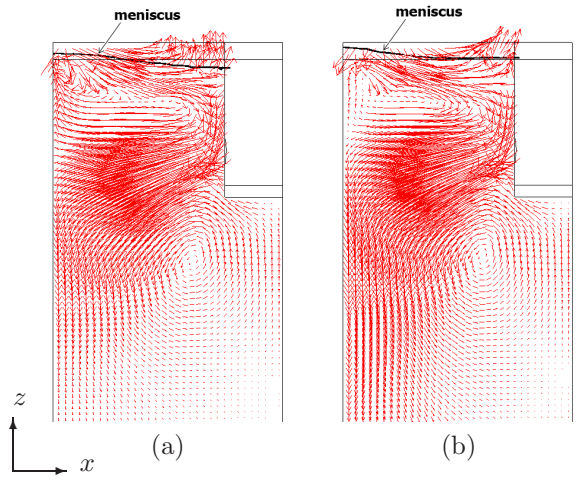

FIGURE 3. Velocity field on a vertical symmetric plane obtained from two different models: (a) with no EM force; (b) with EM force.

the lubricant fluid is pushed into the gap along the mould wall during the downward period of the mould wall, and flows out of the gap during the upward period. Figure 12 presents the variation of the meniscus level at various instants of time during

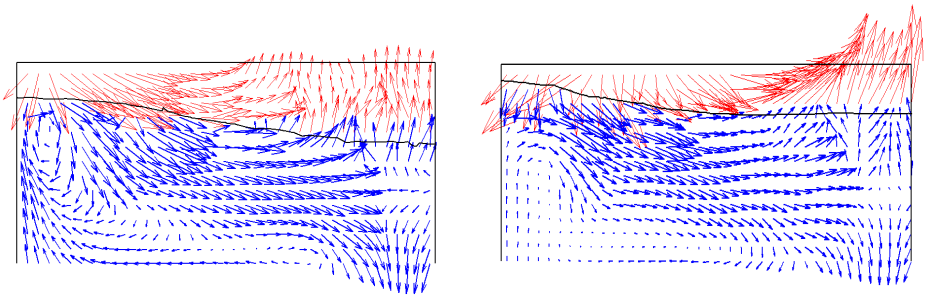

(a) (b)

FIGURE 4. velocity field around the meniscus region under two different cases: (a) with no EM force; (b) with EM force.

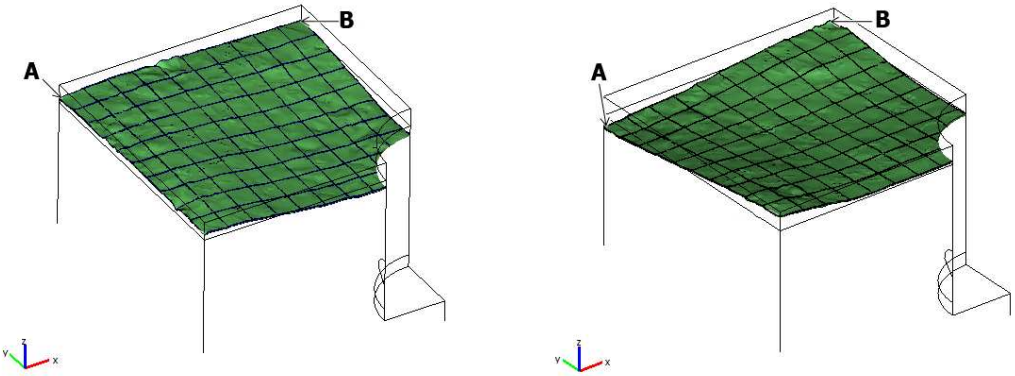

(a) (b)

FIGURE 5. Meniscus surface under two different cases: (a) with no EM force; (b) with EM force.

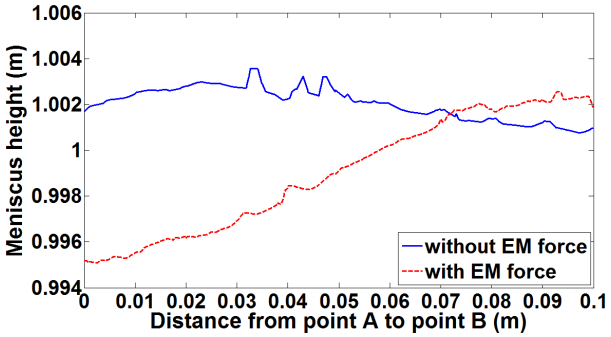

FIGURE 6. Meniscus profile along the mould wall from the billet corner to the symmetry plane.

an oscillation cycle of the mould. It shows that the interface moves away from the

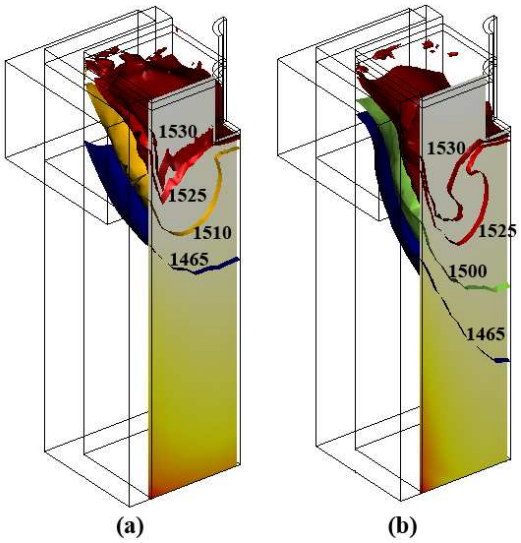

FIGURE 7. Temperature distribution under two different cases: (a) with no EM force; (b) with EM force.

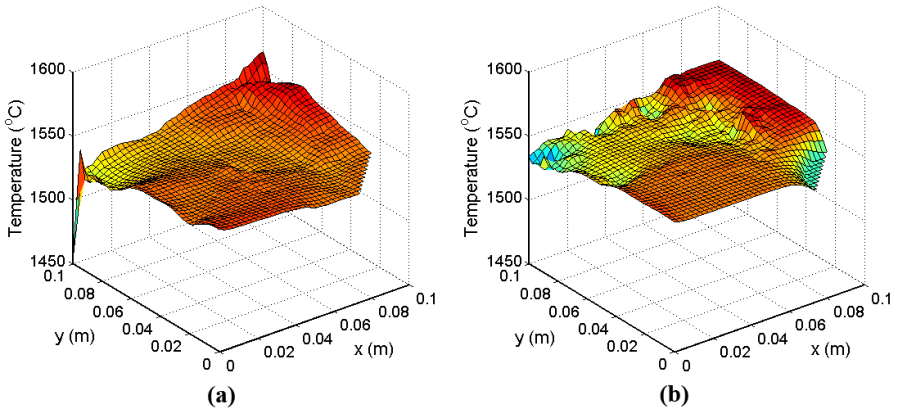

FIGURE 8. Temperature distribution on the meniscus surface under two different cases: (a) with no EM force; (b) with EM force.

mould wall during the downward period of the mould wall, and moves toward the mould wall during the upward period of the mould wall.

Therefore, we can conclude that the EM force and the mould oscillation have significant effect on the solidification process and the movement of the interface between the molten steel and the lubricant fluid. The electromagnetic force can be used to control the velocity field in the mould region to achieve more uniform melt flow in the mould.

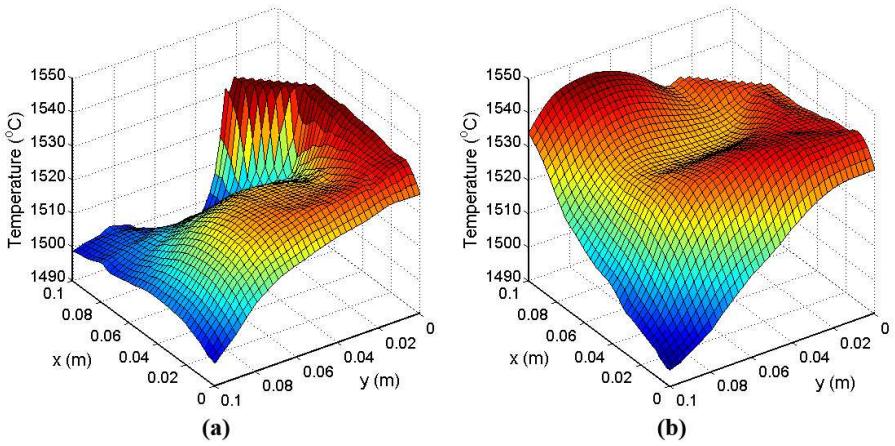

FIGURE 9. Temperature distribution on a horizontal plane ($z = 0.96$) m under two different cases: (a) with no EM force; (b) with EM force.

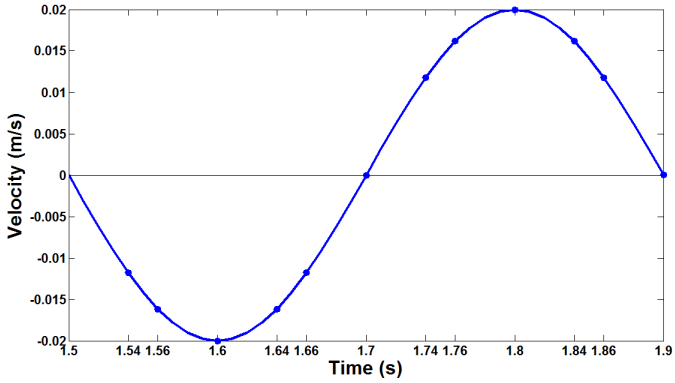

FIGURE 10. Mould oscillation velocity $V = A\cos(\omega t)$, and instants of time for showing the velocity field and meniscus profiles.

Acknowledgments. The first and the second authors gratefully acknowledge the support of the Office of the Higher Education Commission and the Thailand Research Fund through the Royal Golden Jubilee Ph.D. Program (Grant No. PHD/0212/2549). The third author acknowledges the support of an Australia Research Council Discovery project grant.

REFERENCES

[1] J.Archapitak, B. Wiwatanapataphee, Y.H. Wu, *A finite element scheme for the determination of electromagnetic force in continuous steel casting*, Int. J. Computational and Numerical Analysis and Applications, **5**(1) (2004), 81–96.

[2] W.J. Boettinger, S.R. Coriell, A.L. Greer, A. Karma, W. Kurz, M. Rappaz and R. Trivedi, *Solidification microstructure: recent developments, future direction*, Acta Mater, **48** (2000), 43–70.

[3] J.U. Brackbill, D. Kothe, and C. Zemach, *A Continuum method for modeling surface tension*, J. Comput. Phys., **100**, (1992) 335–353.

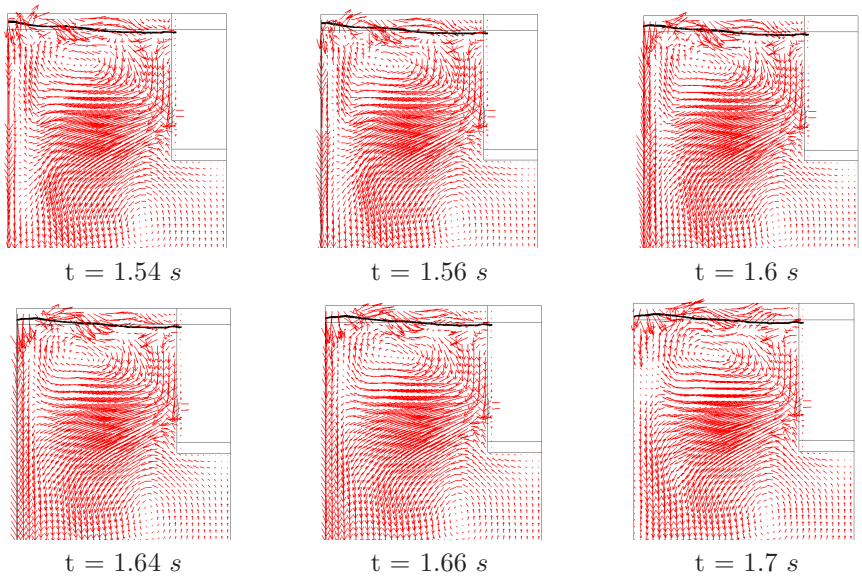

(a) During downward movement of the mould

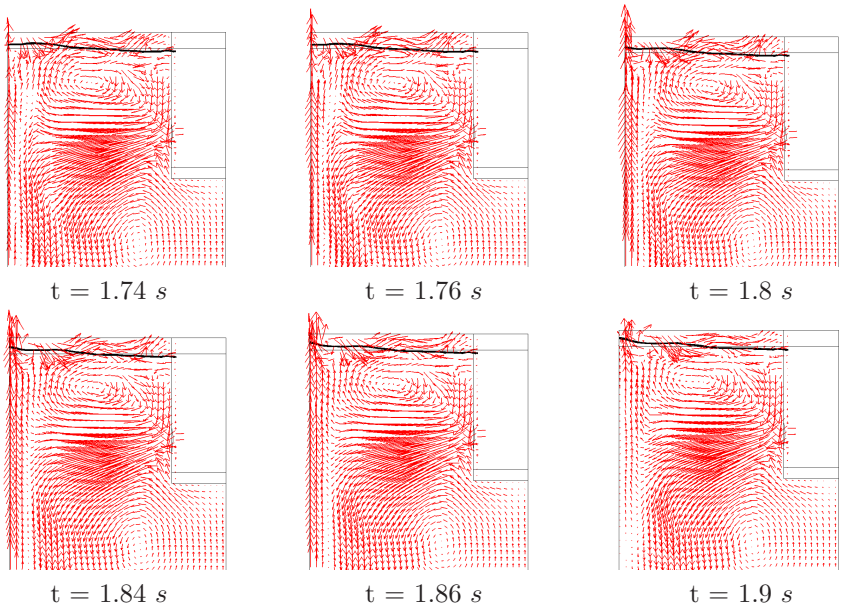

(b) During upward movement of the mould

FIGURE 11. Velocity field of two-fluid flow and meniscus profile at various instants of time during a cycle of mould oscillation (see figure 10 for the instants of time in the mould oscillation cycle).

[4] Y.C. Chang, T.Y. Hou, B. Merriman, and S. Osher, *A level set formulation of Eulerian interface capturing methods for incompressible fluid flows*, J. Comput. Phys., **124**, (1996) 449–464.

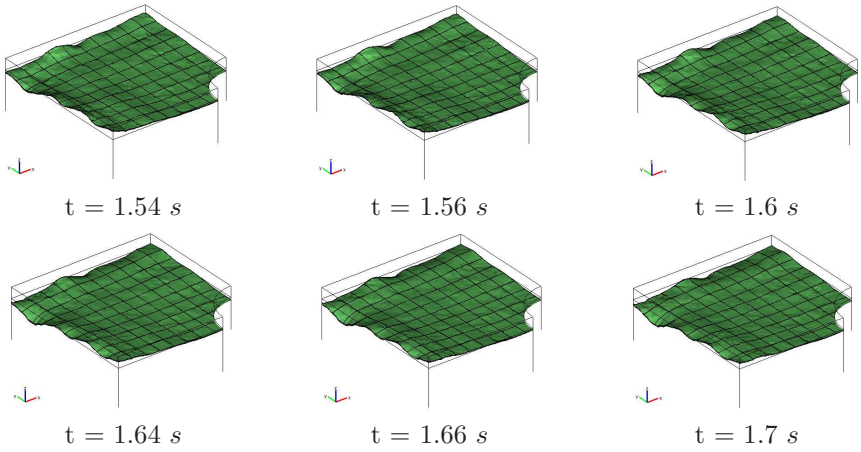

(a) During downward movement of the mould

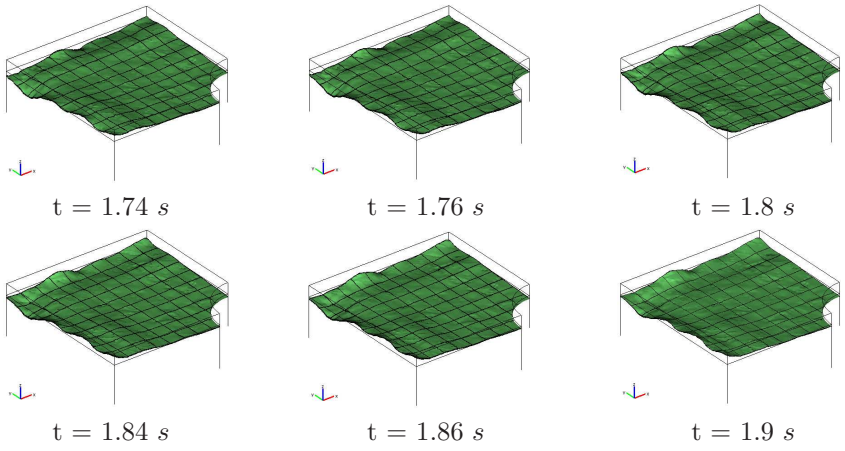

(b) During upward movement of the mould

FIGURE 12. Variation of meniscus shape during mould oscillation.

[5] F. Duarte, R. Gormaz and S. Natesan, *Arbitrary Lagrangian-Eulerian method for Navier-Stokes equations with moving boundaries*, Comp. Methods Appl. Mech. Engrg. **193** (2004), 4819-4836.

[6] J.H.Ferziger, *Simulation of incompressible turbulent flows*, Engineering Mathematics, **36**(4) (1999), 311–326.

[7] V. Girault, H. Lopez and B. Maury, *One time-step finite element discretization of the equation of motion of two-fluid flows*, Numer Methods Partial Differential Eq. **22** (2005), 680-707.

[8] F.H. Harlow and P.I. Nakayama, *Turbulence transport equations*, Phys Fluids, **10**(11) (1967), 2323–2328.

[9] M.D. Gunzburger, "Penalty Methods, Finite Element Methods for Various Incompressible Flows", Academic Press, New York, 1989.

[10] J.M. Hill and Y.H. Wu, *On a nonlinear Stefan problem arising in the continuous casting of steel*, Acta Mechanica, **107** (1994), 183–198.

[11] J.M. Hill, Y.H. Wu and B. Wiwatanapataphee, *Mathematical analysis of the formation of oscillation marks in the continuous steel casting*, Engineering Mathematics, **36**(4) (1999), 311–326.

[12] D.R. Jenkins and De Hoog F.R., *Calculation of the magnetic field due to the electromagnetic stirring of molten steel*, Numerical Methods in Engineering'96, John Wiley and Sons Ltd (1996), 332–336.

[13] A. Karma, *Phase-field formulation for quantitative method of alloy solidification*, Phys Rev. Lett. **8711** (2001), art no. 115701.
[14] H. Kim, J. Park, H. Jeong and J. Kim, *Continuous casting of billet with high frequency electromagnetic field*, ISIJ International, **42**(2) (2002), 171–177.
[15] B. Li and F. Tsukihashi, *Effect of static magnetic field application on the mass transfer in sequence slab continuous casting process*, ISIJ International, **41**(8) (2001), 844–850.
[16] X-Y. Luo, M-J. Ni, A. Ying and M. Abdou, *Application of the level set method for multi-phase flow computation in fusion engineering*, Fusion Engineering and Design, **81** (2006), 1521-1526.
[17] B. Maury, *Characteristics ALE method for the unsteady 3D Navier-Stokes Equations with a free surface*, Comp. Fluid Dyn. **6** (1996), 175-188.
[18] E. Olssen, G. Kreiss, and S. Zahedi, *A conservative level set method for two phase flow II*, J. Comput. Phys., **225**, (2007) 785–807.
[19] U. Pasaogullari and C-Y. Wang, *Two-phase modeling and flooding prediction of polymer electrolyte fuel cells*, J. of The Electromhemical society, **152**(2) (2005), A380-A390.
[20] W. Rodi and D.B. Spalding, *A two-parameter model of turbulence and its application to free jects*, Warme-und Stofubertragung, **3**(2) (1970), 85–95.
[21] P. Sivesson, G. Hallen and B. Widell, *Improvement of inner quality of continuously cast billets using electromagnetic stirring and thermal soft reduction*, Ironmaking & Steelmaking, **25** (3)(1998), 239–246.
[22] B.G. Thomas, Metallurgical Transactions B, **21** (1990), 387–400.
[23] B.G. Thomas, *Continuous casting: modelling*, The Encyclopedia of Advanced Materials (J. Dantzig, A. Greenwell and J. Michalczyk eds), Pergamon Elsevier Science Ltd, UK, 2001.
[24] H.S. Udaykumar, S. Marella and S. Krishman, *Sharp-interface simulation of dendritic growth with convection: benchmarks*, Int. J. Heat Mass Transfer, **46**(14) (2003), 2615–2627.
[25] B. Wiwatanapataphee, Y.H. Wu, A. Jutatip and P.F. Siew, *A numerical study of the turbulent flow of molten steel in a domain with a phase-change boundary*, Journal of Computational and Applied Mathematics, **166**(1) (2004), 307–319.
[26] B. Wiwatanapataphee, *Mathematical modelling of fluid flow and heat transfer in continuous steel casting process*, PhD Thesis, School of Mathematics, Curtin University of technology, Australia, 1998.
[27] Y.H. Wu, J.M. Hill and P. Flint, *A novel finite element method for heat transfer in the continuous caster*, J. Austral. Math. Soc. Ser. B, **35** (1994), 263–288.
[28] Y.H. Wu and B. Wiwatanapataphee, *An Enthalpy control volume method for transient mass and heat transport with solidification*, Int. J. of Computational Fluid Dynamics, **18**(7) (2004), 577–584.
[29] Y.H. Wu and B. Wiwatanapataphee, *Modelling of turbulent flow and multi-phase heat transfer under electromagnetic force*, Discrete and Continuous Dynamical System Series B, **8**(3) (2007), 695–706.
[30] Yi Yang and H.S. Udaykumar, *Sharp interface cartesian method III: Solidification of pure materials and binary solutions*, Journal of Computational Physics, **210** (2005), 55-74.

Received xxxx 20xx; revised xxxx 20xx.

E-mail address: scbww@mahidol.ac.th
E-mail address: t.mookum@gmail.com
E-mail address: yhwu@maths.curtin.edu.au